Femtosecond Dynamics of Interfacial and Intermolecular Electron Transfer at Eosin-Sensitized Metal Oxide Nanoparticles

Serge Pelet,† Michael Grätzel, and Jacques-E. Moser*

Laboratory for Photonics and Interfaces, Institute of Molecular and Biological Chemistry, Ecole Polytechnique Fédérale de Lausanne, CH-1015 Lausanne, Switzerland

Received: October 31, 2002

Photoinduced electron injection from eosin Y into the conduction band of titanium dioxide was further scrutinized, as previous studies on the charge injection from xanthene dyes have led to diverging conclusions. Eosin-sensitized TiO_2 constitutes in many aspects a model system for studying the dynamics of charge injection: Adsorption of the sensitizer onto the oxide surface through electrostatic interaction and hydrogen bonding make this system exemplary of the weak electronic coupling case. The formation of dimeric eosin on the surface of metal oxide nanoparticles in an aqueous suspension was inferred from the study of the deactivation of the dye's singlet excited state on insulating particles, such as ZrO_2 and Al_2O_3, and of the formation of the resulting radical ion pair, using femtosecond stimulated emission and transient absorption. It was found that dimers undergo ultrafast dismutation with a time constant of 500 fs. The same process occurs also on TiO_2 particles and results in a competition between interfacial and intermolecular electron transfer. Two time constants of 160 fs (58%) and 1 ps were obtained for the charge injection from the singlet excited state of eosin into this semiconductor. The presence of poly(vinyl alcohol), often used as a stabilizer for aqueous colloidal suspensions, was observed to prevent the dimer formation on the surface but also to slow the rate of electron injection by orders of magnitude. This observation is rationalized in terms of an increased distance between the semiconductor surface and the chromophore because of the adsorption of polymeric chains onto the particles and a decrease of the electronic coupling matrix element associated to the charge transfer process. These findings remove the apparent discrepancies perceived between early measurements and more recent reports and highlight the role played by the mode of adsorption of the sensitizer in controlling electron injection kinetics.

I. Introduction

Light-induced electron injection from molecular dyes into the conduction band of wide-band gap semiconductor nanoparticles is currently intensely studied. This process is at the base of numerous technical applications, such as silver photography,[1] xerography,[2] and molecular photovoltaics,[3,4] which rely on the redox sensitization of semiconducting materials. From a fundamental standpoint, electron transfer from the excited state of a donor molecule to a continuum of electronic acceptor states in a solid also has significant importance. Classical theoretical treatments for electron transfer (ET) [5] and further quantum mechanical extensions [6] are based on the assumption that the energies of the donor and acceptor states are matched by energy fluctuations caused by the thermal bath and thus that the overall ET kinetics is controlled by the nuclear activation barrier to achieve electronic resonance between reactant and product states. A fundamentally different situation is found in sensitizer/semiconductor systems, where charge injection takes place from an excited molecular state into a wide continuum of acceptor levels constituting the conduction band of the solid. In this case, the rate constant for interfacial ET should only be controlled by electronic interaction without much influence of Franck−Condon factors.[7,8]

Recent ultrafast studies have shown charge injection from excited dye molecules in the conduction band of oxide semiconductors to occur in the femtosecond time domain.[9−19] The time constant for ET has been found in these studies to vary from 6[13] to 500 fs.[14] Charge-transfer times of 50 fs indicate that the corresponding electronic coupling strengths are approaching the value of the thermal energy kT ($\sim$ 200 cm^{-1}) and, thus, that the reactions are likely to have reached the adiabatic limit.[20] The notion that the electron is transferred to the solid well before vibrational relaxation of the excited sensitizer has recently been confirmed in strong coupling cases by the observation of the dependence of ET kinetics upon the excitation photon energy[21−23] and that of oscillations in the transient absorption signal due to vibrational wave packet motion during heterogeneous charge transfer.[24,25] The strong electronic coupling prevailing for an efficient sensitizer is generally the result of the anchoring of the dye molecule onto the semiconductor surface through a moiety carrying its LUMO.[20] This situation is clearly encountered in carboxylated Ru(II) polypyridyl complexes,[10] porphyrin,[26] coumarin,[9,11] or anthracene [15,17] dyes, for example. Hydroxy-quinoline,[27] ferrocyanide,[28−30] phenylfluorone,[31] squarain,[32] and alizarin [12,33] represent extreme cases in this respect, as these chelating molecules form charge-transfer complexes with acidic surface metal cations, giving rise to new chromophoric species.

The electronic coupling can be diminished by increasing the distance separating the LUMO of the dye from the surface of

* To whom correspondence should be addressed. Phone: +41 21 693 3628. Fax: +41 21 693 4111. E-mail: je.moser@epfl.ch.

† Present address : Department of Mechanical and Biological Engineering, Massachusetts Institute of Technology, Cambridge, MA 02139.

10.1021/jp027358x CCC: $25.00
Published on Web 03/12/2003

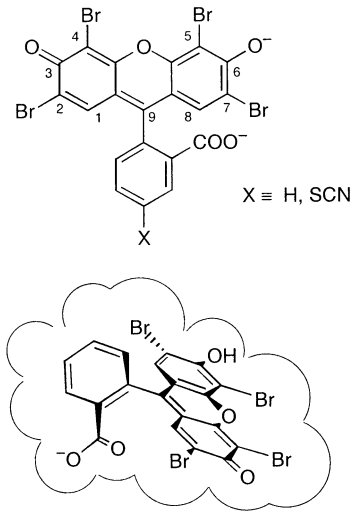

Figure 1. Chemical structure of the anionic form of eosin Y (EO, X ≡ H) and eosin-5-isothiocyanate (X ≡ NCS). 3-D structure was obtained from a MOPAC semiempirical quantum mechanical calculation. Arcs drawn around the molecule represent van der Waals overall dimensions of peripheral atoms.

the semiconductor material. This can be achieved by inserting insulating spacer units between the chromophore and the anchoring group. Lian and co-workers have studied the bridge-length dependence of ultrafast charge injection from rhenium-polypyridyl complexes to nanocrystalline TiO_2 films and have suggested that the transition between the strong- (adiabatic) and weak coupling (nonadiabatic) cases takes place for transfer distances increased by only one $-CH_2$ unit length (~3 Å).[19] A comparable decrease of the donor−acceptor electronic coupling is also likely to occur with sensitizer molecules loosely associated to the semiconductor charged surface by electrostatic interaction and/or hydrogen bonding. In aqueous medium, the surface of oxides is hydroxylated. Large sensitizer ionic species, which are thermodynamically unable to displace hydroxyl groups and adsorb within the Helmoltz layer, should hence be maintained several angstroms apart from the solid.

In acidic medium, amphoteric oxides are characterized by a positively charged surface that allows for the preparation of stable colloidal suspensions of nanocrystallites. Among anionic sensitizers liable to adsorb on the semiconductor particles in these conditions, xanthene dyes were early recognized as choice systems: Moser, more than a century ago, observed that erythrosin (2′,4′,5′,7′-tetraiodofluorescein) could significantly enhance the spectral response of a photovoltaic cell based on silver halide electrodes.[34] The first time-resolved studies of the charge injection process were reported for erythrosin and eosin Y (2′,4′,5′,7′-tetrabromofluorescein, Figure 1) adsorbed on colloidal TiO_2.[35−37] For the latter dye in solution, a wealth of spectroscopic, kinetic, and thermodynamic data is available in the literature (see [37] and references therein). Well resolved absorption spectra of the various transient species and significant luminescence of the excited state, moreover, allow for a rather easy monitoring of the dynamics of the photoinduced interfacial electron-transfer reaction in eosin/metal oxide model systems.

Early nanosecond laser studies of eosin adsorbed on aqueous colloidal TiO_2 were not able to resolve the injection process kinetics. However, they showed that the singlet excited state was sufficiently long-lived to permit partial intersystem crossing.[37] Measurements of the respective fluorescence, triplet, and injection quantum yields ($\Phi_f = 0.09$, $\Phi_T = 0.18$, $\Phi_{inj} = 0.38$), combined with a reported value of the radiative decay rate constant $k_r = 1.9 \times 10^8\ s^{-1}$,[38] allowed us to determine indirectly a rate constant $k_{inj} = 8.5 \times 10^8\ s^{-1}$ for photoinduced interfacial ET at pH 4 and in the presence of poly(vinyl alcohol).[37] Further experiments carried out in the same conditions with picosecond time resolution confirmed this finding in establishing directly the dye's singlet excited-state lifetime $\tau = 380 \pm 40$ ps and the rate constant for the appearance of the eosin semioxidized radical $k_{inj} = (9.5 \pm 1.4) \times 10^8\ s^{-1}$.[39]

Studies by Sundström and co-workers that employed femtosecond time-resolution and the parent dye molecule 2′,7′-dichlorofluorescein adsorbed on TiO_2 have questioned these early results, as quantitative injection and time constants ranging from <100 fs to ca. 8 ps were observed.[16,40,41] Also notable in this work were the reported large changes of the dye absorption spectrum upon adsorption onto colloidal TiO_2 particles, which was interpreted as being due to the strong association of the carboxylic group of the fluorescein sensitizer with surface Ti(IV) ions through the formation of a bidentate surface complex.[16] This notion was further amplified by Ramakrishna and Ghosh who construed steady-state absorption spectra of various xanthene dyes adsorbed on titania nanoparticles as being indicative of the formation of surface charge-transfer complexes.[42] The latter conclusion was finally refuted recently by Hupp et al., whose Stark emission spectroscopy experiments revealed that eosin Y injects via a locally excited state with no significant interfacial charge-transfer character.[43]

In view of these contradictory results, we have carried out further detailed experimental studies with eosin in aqueous solution and adsorbed on TiO_2 colloidal particles, which we present in this paper. ZrO_2 and Al_2O_3 colloids will be used as reference systems as eosin is expected to be associated with the acidic surface of these oxides and that of titania in a very similar fashion. The conduction band edges of zirconia and alumina, however, are set at respective energies more than 1 and 2 eV higher compared to that of TiO_2, thus making charge injection from the eosin excited state into these two materials thermodynamically unfeasible. For simplicity, the anionic form of eosin will be referred in the following as EO. Semioxidized and semireduced radicals will be designated by $EO^{+\bullet}$ and $EO^{-\bullet}$, respectively, irrespective of the degree of protonation of these species.

II. Experimental Section

Materials. Eosin Y disodium salt (Fluka) was purified by column chromatography and repeated recrystallization of its protonated form in water.[37] Eosin-5-isothiocyanate (Fluka) was used as supplied by the vendor. Ultrapure deionized water was prepared with a Milli-Q system (Millipore). TiO_2 and ZrO_2 aqueous colloidal suspensions were prepared by the hydrolysis of vacuum-distilled $TiCl_4$ and $ZrCl_4$, according to a common procedure previously reported for titania.[44] The hydrodynamic diameter of the oxide particles was 10−20 nm, as measured by photon correlation spectroscopy. Ludox CL aqueous alumina colloid was purchased from Aldrich. This was constituted of SiO_2 core particles covered by an Al_2O_3 layer. Typical particle size was 50 nm. The three oxide colloidal stock solutions were diluted by pure water to reach a concentration of 5 g/L at pH ≈ 3. Poly(vinyl alcohol) (PVA) (Mowiol 10-98, MW ≅ 48,000, 98% hydrolyzed,) was obtained from Clariant. The polymer was dissolved in water and added in some cases to TiO_2 colloidal suspensions at a concentration of 1 g/L to obtain PVA-protected particles. The purified neutral protonated eosin was solubilized in alkaline water (pH = 9, NaOH) at a concentration of 10^{-3} M. Small volumes of the concentrated dye solution were added

progressively to colloidal oxide suspensions (5 g/L) to reach typically a final sensitizer concentration of 5×10^{-5} M. The pH of the solutions was finally adjusted at a value of 4.0 with HCl and/or NaOH solutions. All dye-sensitized colloids were equilibrated overnight prior to be used. Dyed suspensions stored in the dark were transparent and stable for weeks.

Femtosecond Transient Spectrometer. Time-resolved transient absorption and stimulated emission measurements by the pump−probe technique used a compact CPA-2001, 1 kHz, Ti:Sa-amplified femtosecond laser (Clark-MXR), with a pulse width of about 120 fs and a pulse energy of 1 mJ at a central wavelength of 775 nm. The output beam was split into three parts for pumping two double-stage noncollinear optical parametric amplifiers (NOPA) and to produce a white light continuum in a sapphire plate or 387 nm UV light by second harmonic generation of the CPA output in a thin BBO crystal. NOPAs were based on the design published by Piel et al.[45] Both amplifiers were pumped by 200 μJ pulses at a central wavelength of 775 nm and were continuously tunable over a wide wavelength range extending from 450 to 1700 nm. The NOPA used for exciting the sample was set to provide pulses of approximately 10 μJ energy at a central wavelength of 500 nm. The second NOPA was tuned either at 600 or 480 nm, yielding approximately the same energy. The output pulses of the NOPAs were compressed in SF10-glass prism pair compressors down to a duration of less than 30 fs (fwhm). Iris diaphragms were used to decrease the pulse energy down to a few microjoules for the pump and to less than 1 μJ for the probe beam. Polarization between both beams was controlled using a coherent zero-order half waveplate, and experiments were carried out at the magic angle (54.7°) configuration. Pump and probe beams were directed parallel to each other toward a 60° off-axis paraboloid mirror that focused them into the sample. The cross-correlation measured by Kerr gating in a 0.3-mm-thick PBH21 glass window (Ohara) at the sample position was typically 80 fs (fwhm).

In the case of monochromatic probing, a DET-110 silicon diode (Thorlabs), placed directly after the sample, was used to measure the transmitted light intensity. An iris diaphragm and suitable filters blocked the contribution from the pump beam. The signal from the detector was sent to a SR-830 lock-in amplifier (Standford Research Instruments) tuned at the frequency (220 Hz) of a chopper modulating the pump beam. Time delays between pump and probe pulses were controlled by two linear translation stages (Aerotech Unidex 100M and Physik Instrumente M511) placed on the paths of the two respective beams. The signal measured from the lock-in amplifier at a given time delay was assumed to be proportional to the transmittance change experienced by the sample upon laser excitation and further reaction.

Transient spectra were measured using a white light continuum (WLC) for probing. The latter was generated from pulses (energy <10 μJ) focused into a 2 mm thick sapphire plate. The monofilament white beam was collimated using a 90° off-axis paraboloid mirror and steered to the sample using only reflective optics. A smooth monotonic spectral distribution between 470 and 670 nm was obtained by controlling the pump energy with an iris and a variable density filter. Chirped pulse duration was less than 400 fs as measured by Kerr gating in PBH21 glass.[46] A broadband membrane-beam splitter was placed before the sample to split the probe beam into reference and signal arms. Both were collected by fiber bundles and sent to a Triax 320 spectrograph (Jobin-Yvon). Reference and signal beams were separated vertically during their travel in the spectrograph and were detected individually by a ST116 double diode array detector (Princeton Instruments). Both 1024 elements detector arrays allowed for recording more than 200-nm-wide spectra at a time. At each time delay, spectra were measured by averaging over approximately 10^5 laser shots. The absorbance change was calculated using the ratio between data obtained with and without the pump pulses reaching the sample and corrected for fluctuations in the WLC intensity using the reference beam spectra.

Liquid samples were placed in a 1 mm pathway optical cell, consisting of two thin microscope coverglass windows separated by a PTFE spacer. Two actuators were used to move continuously the sample in a plane perpendicular to the pump and probe beams during data acquisition. A *Labview* program (National Instruments) was written to interface the lock-in amplifier, the double diode array, and the delay lines, allowing for fully automated data acquisition. Fitting of data to the desired mathematical functions was achieved using *IgorPro* routines (Wavemetrics Inc.), based on Marquardt-type nonlinear optimizations.

Other Methods. Steady-state absorption spectra were recorded on an HP-8353 (Hewlett-Packard) or a Cary 5 (Varian) spectrophotometer. Emission measurements used a Fluorolog 2 spectrofluorometer (Jobin-Yvon Spex). All reported fluorescence spectra were corrected for spectral detection response. Colloidal suspensions prepared for transient absorption experiments were further diluted 20 times (2.5×10^{-6} M dye on 0.25 g/L colloid) and acidified by HCl to reach pH 4 prior to absorption and fluorescence characterization. Electrophoretic mobilities of TiO_2 particles were measured with a Mark II apparatus (Rank Bros), equipped with a 5 cm quartz cylindrical cell. An ultra-microscope system constituted of a green diode-pumped, frequency-doubled, Nd:YAG laser and a CCD camera allowed for the visualization of the moving individual nanoparticles. The pH of dilute solutions containing 25 mg/L titanium dioxide colloid was adjusted to different values using HNO_3 and KOH solutions. The ionic strength was kept constant by adding 10^{-3} M KNO_3 to all measured samples.

III. Results

The characterization of the dye-colloidal system by steady-state spectroscopy was carried out with 2.5×10^{-6} M EO solutions. When solutions contained colloidal oxide particles, the concentration of the solid was 0.25 g/L. The fluorescence experiments could not be realized with more concentrated solutions because of light scattering by particles and high extinction of the dye. Assuming quantitative adsorption of the dye onto the available surface, the average number $\langle z \rangle$ of dye molecules adsorbed per 10 nm diameter particle was estimated to be 100.[37] This ratio was identical for more concentrated solutions (5×10^{-5} M EO, 5 g/L colloid) submitted to transient laser spectroscopy, and the absorption spectra of these solutions yielded indeed similar results. The pK_a of the phenolic and carboxylic groups of EO in aqueous solution were reported to be 4.4 and 3.4, respectively,[37] which means that at pH 4, dye molecules are partly protonated and are present mainly in their monoanionic form. As shown in Figure 2A, EO in acidic aqueous solution is characterized by a sharp absorption in the visible with a maximum at 520 nm. ZINDO semiempirical quantum mechanical calculations carried out using *CAChe WorkSystem* program package (Fujitsu) show that this transition is of $\pi-\pi^*$ character, with the HOMO distributed on the xanthene fused ring part and the LUMO localized on the carbon atom in position 9′. Optimization of the molecule geometry by *CAChe* MOPAC-2002 program indicates that the benzoic ring

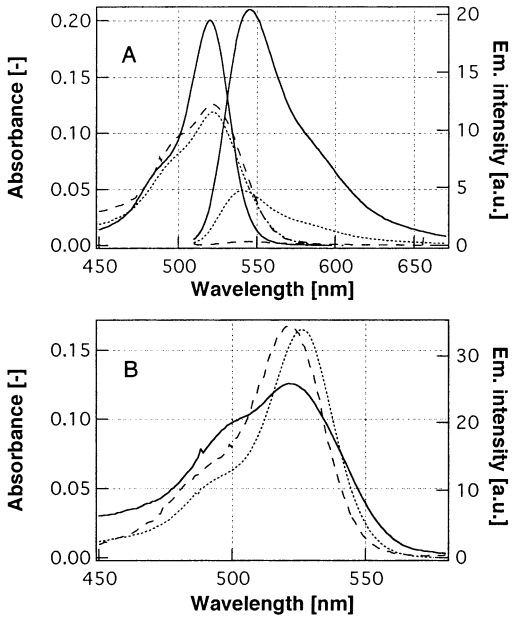

Figure 2. (A) Absorption and emission spectra of EO 2.5×10^{-6} M in aqueous solution at pH 4 (—), and adsorbed on unprotected TiO_2 (- - -) and ZrO_2 (•••) colloids (0.25 g/L). (B) Absorption spectra of EO adsorbed onto PVA-protected (•••) and unprotected (—) TiO_2 colloids and fluorescence excitation spectrum of the unprotected sensitized colloid in identical conditions (- - -).

moiety is rotated perpendicular to the xanthene plane (Figure 1), thus making the coupling of the carboxylic group with the chromophore unlikely. The fluorescence spectrum of eosin is the mirror image of the absorption with a minor 720 cm^{-1} Stoke's shift, indicating similar ground and excited-state geometries. The fluorescence lifetime $\tau < 1$ ns is limited by efficient intersystem crossing ($\Phi_T = 80\%$), because of the presence of four bromine heavy atoms.[47] Eosin-5-isothiocyanate derivative was used for comparison. Despite the presence of such an electron donating substituant on the benzoic moiety, absorption and fluorescence spectra of this compound are identical to those of plain eosin.

Upon adsorption onto TiO_2, ZrO_2, and Al_2O_3 particle surfaces at constant pH, the absorption spectrum of eosin is observed to be modified (Figure 2). The oscillatory strength decreases and a shoulder appears on the blue side of the main peak at ca. 490 nm. A similar feature was observed by Benkö et al. upon adsorption of 2′,7′-dichlorofluorescein on titania films.[41] The shape of the eosin emission spectrum, nevertheless, remains basically unaffected by adsorption on the three oxide materials. The fluorescence intensity is decreased by a factor of 50 in the presence of TiO_2 particles. A significant quenching of the fluorescence down to ca. 20% of the original intensity is also observed upon adsorption of EO on ZrO_2 and Al_2O_3.

Figure 2B compares the absorption spectra of eosin adsorbed on PVA-protected and unprotected TiO_2 colloids. Addition of 1 g/L poly(vinyl alcohol) suppresses the 490 nm shoulder on the dye spectrum. The absorption maximum of the EO/PVA/TiO_2 system exhibits only a small red shift of 6 nm over that of the free dye in water. The excitation spectrum also shows that the emissive species for EO adsorbed on TiO_2 is spectrally similar to the anionic form of the dye in water and lacks the shoulder on the blue side of the absorption peak.

Microelectrophoresis measurements employed 25 mg/L TiO_2 colloids. These very dilute sols were stable enough to allow for the determination of the point of zero charge of unprotected particles (PZC) without noticeable precipitation in critical pH

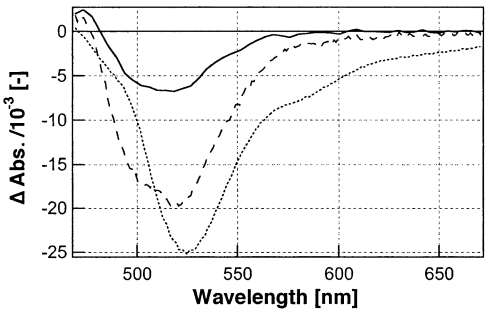

Figure 3. Transient absorbance spectra of EO 2×10^{-5} M recorded 10 ps after pulsed excitation in water (divided by 5) (•••) and in Al_2O_3 colloid (5 g/L) (- - -), as well as of eosin adsorbed on unprotected TiO_2 colloid (5 g/L) (—) measured 200 ps after laser excitation at 500 nm.

conditions. The measured mobility of the bare oxide nanoparticles established at a value of $u = 3.8$ m^2 V^{-1} s^{-1} at pH 4. This figure, translated in terms of surface zeta potential by application of Henry's law, corresponds to a positive surface charge with $\zeta = 82$ mV. The point of zero charge of the oxide was found at pH 5.0. The latter values are significantly lower than the ones reported for purified, fully hydroxylated, anatase particles ($\zeta = 94$ mV, PZC = 6.2) in similar conditions.[48] This difference is likely to be due to the contamination of the colloidal particles by chloride ions trapped in the material during its preparation from $TiCl_4$.[44] Specific adsorption of ions onto a surface can indeed be recognized by two effects: (a) it causes a shift in the point of zero charge of the particles as the concentration of the adsorbate is increased and (b) it alters the surface zeta potential of the solid and can even revert its sign when specifically adsorbed ions are present at high enough concentration. Addition of eosin dye in the sol and subsequent adjustment of the pH value was followed by equilibration in the dark for at least 3 h prior to carrying out electrophoretic measurements. Increasing concentrations of EO from 2.5×10^{-7} M, corresponding approximately to $\langle z \rangle = 10^2$ EO molecules per TiO_2 nanoparticle, up to 10^{-5} M ($\langle z \rangle = 4 \times 10^3$) did not cause the mobility to deviate significantly from the value determined for the bare oxide. At concentrations [EO] $\geq 10^{-6}$ M ($\langle z \rangle \geq 400$), the fluorescence of the dye was observable by eyes, indicating that adsorption reached the saturation of the available oxide surface and that a major part of the sensitizer was actually present in solution. In these conditions, ζ (p*H* 4) = 78 mV and again PZC = 5.0 were measured. Electrophoretic measurements were also carried out with TiO_2 sols (25 mg/L) in which 5 mg/L poly(vinyl alcohol) was adjoined. In the absence of eosin, the point of zero charge of PVA-protected nanoparticles was found to remain unchanged at a value of PZC = 5.0. Zeta potential, however, decreased markedly down to ζ(pH 4) = 42 mV. Addition of 10^{-5} M eosin to titania colloids already equilibrated in the presence of a PVA adlayer did not produce any change in electrophoretic data.

Figure 3 shows the transient absorption spectra of eosin in aqueous solution at pH 4 and in the presence of a TiO_2 colloid, recorded respectively 10 and 200 ps after pulsed laser excitation. The negative absorption change observed for free aqueous EO between 470 and 550 nm can be attributed to the bleaching of the ground state of the dye upon excitation at 500 nm. Stimulated emission (SE) from EO singlet excited-state yields also an apparent negative absorbance change in the 550−670 nm region. When eosin is adsorbed on TiO_2, quenching of the fluorescence through electron injection prevents any observation of such a signal 200 ps after excitation. However, a positive absorption appears below 480 nm that can be unambiguously

TABLE 1: Polyexponential Fitting Parameters of Eosin Dynamics Measured in Different Media

medium	$\lambda = 600$ nm	$\lambda = 480$ nm	$\lambda = 387$ nm
H_2O, pH 4	85 ± 25 fs (66%, growth)		
	1 ± 0.5 ps (34%, growth)		
	580 ± 100 ps (decay)		
Al_2O_3 colloid	490 ± 40 fs (77%)	580 ± 150 fs (34%)	
			12 ± 3 ps (74%)
	550 ± 200 ps (33%)		140 ± 120 ps (26%)
ZrO_2 colloid	800 ± 70 fs (52%)		
	210 ± 20 ps (48%)		
TiO_2 colloid	160 ± 50 fs (58%)	280 ± 120 fs (43%)	220 ± 80 fs (53%)
	960 ± 190 fs (42%)	1.9 ± 1.2 ps (28%)	
		19 ± 5 ps (29%)	13 ± 2 ps (47%)
PVA/TiO_2 colloid	1.1 ± 0.3 ps (36%)	1.4 ± 0.4 ps (37%)	
	12 ± 4 ps(34%)	14 ± 3 ps (63%)	
	110 ± 40 ps (30%)	500 ± 600 ps	

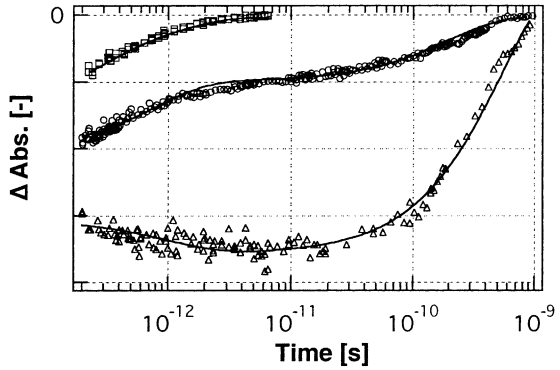

Figure 4. Transient stimulated emission of EO 2×10^{-5} M measured at 600 nm upon excitation at 500 nm. Solid lines represent poly-exponential fits of the experimental data obtained for the dye in solution (△), and adsorbed on TiO_2 (□) and ZrO_2 (○) colloids.

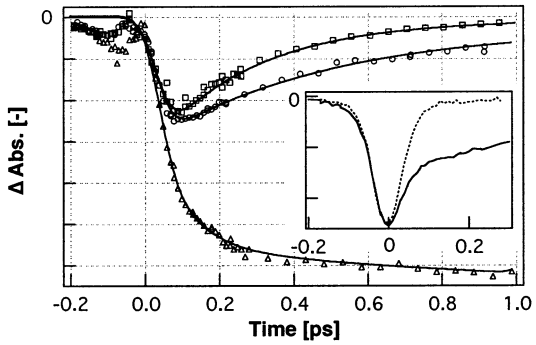

Figure 5. Rise of the stimulated emission at 600 nm measured upon femtosecond excitation at 500 nm of eosin 5×10^{-5} M in water (△), and adsorbed on TiO_2 (□) and Al_2O_3 colloids (○). The inset compares the experimental response from EO on colloidal Al_2O_3 (—) and from pure water (···). The solvent response was subtracted from the data to allow for the fitting by convolutions of a Gaussian and poly-exponential functions, represented by solid lines in the main graph.

assigned to the dye oxidized state $EO^{+\bullet}$.[12,37] Surprisingly, both features are equally observed in the transient spectrum measured at a time delay of 10 ps with eosin adsorbed on nonreactive alumina particles. Although clearly observable, stimulated emission signal is weaker than for EO in solution and the transient positive absorption signal visible only at wavelengths shorter than 475 nm.

The temporal behavior of the stimulated emission (SE) signal from EO was measured at a probe central wavelength of 600 nm following laser excitation at 500 nm (Figure 4). In solution, a rise of this signal was observed in the first picoseconds, which is the result of the cooling of the excited state from a higher Franck−Condon level. At longer delays, the SE signal finally decays because of intersystem crossing and/or ground state recovery. The lifetime of the singlet state was estimated from these data as being $\tau = 580$ ps. Similar dynamics were measured while following either the ground-state bleaching at 480 nm or the singlet−singlet excited-state absorption at 387 nm. Compared to the 1 ns fluorescence lifetime reported in the literature,[47] the measured τ appears shorter. The difference could probably be accounted for by the protonation of the phenolic group of the dye in our experimental conditions.

Upon adsorption of eosin onto TiO_2, the SE signal disappears within less than 10 ps. This result was indeed expected from the low steady-state fluorescence yield. The absence of a long lasting tail in the stimulated emission indicates that only adsorbed sensitizer molecules undergoing efficient electron injection are probed and that free dye anions in solution have only a negligible contribution. The dynamics measured on ZrO_2 shows clearly that two reactions with very different rates take place from the singlet excited state of the dye: An ultrafast process with dynamics similar to what was observed on TiO_2, and a slower one which resembles the natural decay of the singlet state. The solid lines on the graphs represent polyexponential fits of the experimental data. The time constants and amplitudes for each fit are summarized in Table 1.

Figure 5 compares the rise of the stimulated emission of eosin in different media. The inset shows that the aqueous solvent is responsible for a strong coherent spike observed in the raw data. This artifact was subtracted and data were fitted with a convolution of a Gaussian (88 fs fwhm) and a mono- or double-exponential up to a few picoseconds. For eosin on TiO_2 and Al_2O_3, the best fits yielded a single-exponential decay with 270 ± 10 and 480 ± 2 fs half-lifetimes, respectively. In colloid-free solution, the rise of the SE signal due to the cooling of the excited state was observed on a short time scale. Deconvolution yielded two time constants of 85 ± 25 fs and 1 ± 2.5 ps. The large uncertainty on the second value is due to the lack of experimental data beyond 1 ps. The same transient shown in Figure 4 provides a more definite 1 ± 0.5 ps time constant (Table 1).

The dynamics of eosin on Al_2O_3 colloid was measured at various probe wavelengths to follow the different species involved in the deactivation of the excited state in this nonreactive system (Figure 6). At the probe wavelength of 600 nm, the stimulated emission of the singlet excited state displays clearly a biphasic temporal decay with 490 fs and 550 ps time constants. At 480 nm, both the bleaching of eosin ground-state and the absorption of the oxidized species $EO^{+\bullet}$ contribute to the signal. The fitting of the overall signal required at least three exponentials with 580 fs, 18 ps, and 220 ps time constants. At 387 nm, the singlet excited state of eosin and its semireduced form $EO^{-\bullet}$ have similar absorption cross sections.[49,50] The

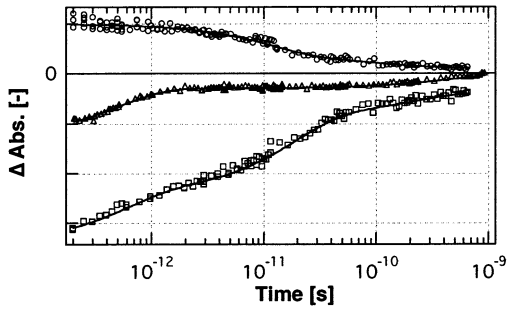

Figure 6. Transient absorbance from eosin adsorbed on Al_2O_3 colloid upon excitation at 500 nm. Probing central wavelengths were 387 (○), 480 (□) and 600 nm (△). The solid lines represent multiexponential fits of the experimental data.

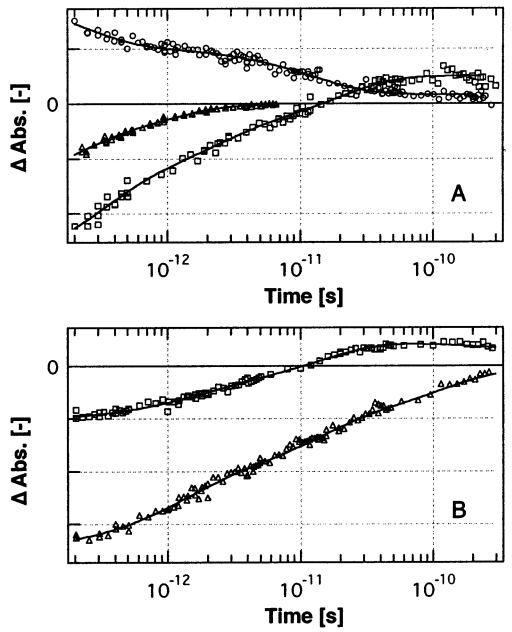

Figure 7. (A) Transient absorbance from eosin 5×10^{-5} M on unprotected TiO_2 colloid (5 g/L) pumped at 500 nm and probed at 387 (○) and 480 nm (□), and stimulated emission of EO at 600 nm (△). (B) Transient absorption from EO 5×10^{-5} M on PVA-protected TiO_2 colloid measured at 480 nm (□) and 600 nm (△) upon femtosecond excitation at 500 nm.

appearance of $EO^{-\bullet}$ could result from a singlet−singlet reaction and will be discussed below. The decay of the transient absorption in the near UV follows biphasic kinetics in the picosecond time frame with 12 and 140 ps time constants. Details of the fitted kinetic constants are provided in Table 1.

The same set of three wavelengths was used to probe the EO/TiO_2 system. Figure 7A shows that at 480 nm the negative transient absorption because of the bleaching of the ground-state evolves into a positive absorbance change due to the formation and absorption of the oxidized species. Three time constants of 280 fs, 1.9 ps, and 19 ps (see Table 1) could be extracted from the overall signal. The dynamics of the singlet excited state should reflect in the stimulated emission signal measured at 600 nm, as well as in the transient absorption probed at 387 nm. A clear difference between both temporal traces was however observed. Although stimulated emission signal decayed promptly in the subpicosecond time scale, the kinetics measured in the UV displayed a slower 13 ps component. This difference between both transients could be rationalized by the formation of the semireduced $EO^{-\bullet}$ species whose absorbance contributes to the signal at 387 nm. Figure 7B demonstrates that the dynamics of eosin is strongly modified by the presence of poly(vinyl alcohol) in the sol. The singlet excited state of eosin is obviously much more long-lived than for the dye associated to unprotected TiO_2 particles. Yet, the stimulated emission signal decay cannot be described by a single exponential and, therefore, does not reduce to the case of free eosin in solution. Transient absorbance monitored at 480 nm shows indeed that PVA does not inhibit the formation of $EO^{+\bullet}$ oxidized species, because a positive absorption feature is observed at delay times exceeding 10 ps.

IV. Discussion

Mode of Adsorption. Early experiments demonstrated that eosin is efficiently associated to the surface of oxide particles in acidic aqueous medium.[37] Spectroscopic data presented in this work show that the adsorption is accompanied by a modification of the absorption spectrum of the sensitizer, and similar observations were reported for other xanthene dyes.[16,41,42] The interpretation of these spectral changes and the assessment of the type of interactions coupling the dye molecules onto the oxide surface have been under debate. Ramakrishna and Ghosh recently invoked the formation of charge-transfer complexes (CT) between xanthene dyes and the surface of titania aqueous colloids, relying on the observation of a marked increase of the absorption of the dye in the presence of the oxide over the corresponding aqueous acidic solution and of a red-shift of both absorption and fluorescence spectra.[42] This conclusion is quite astonishing for different reasons: The optimized 3-D geometry of eosin shows that the carboxylic group of the molecule, which is believed to be responsible for the anchoring of the dye onto the solid surface, is actually decoupled from the chromophoric part of the molecule. This should also be true for other xanthene dyes, in which the benzoic ring has no way to be conjugated with the π orbitals set of the xanthene moiety. In such conditions, complexation of surface Ti(IV) ions by the carboxylic group of the sensitizer should not affect the nature of the HOMO−LUMO transition. A tripod configuration of the anchored molecule, where the keto−enolic oxygen atoms that belong to the chromophore would be in direct contact with titanium atoms of the semiconductor, has been suggested by Hilgendorff and Sundström[16] and would constitute an alternative explanation for the spectral change upon adsorption of the dye. In the particular case of eosin, however, molecular models suggest that bulky bromine substituants in the 4′ and 5′ positions sterically preclude the linkage of the dye in the tripod configuration. Electrophoretic measurements show that adsorption of EO anions as far as to the saturation of the positively charged surface of TiO_2 in acidic aqueous medium does not produce much of a change in the surface ζ potential nor in the isoelectric point of the nanoparticles. The extent of the effect of adsorption of eosin is inferior or comparable to what has been observed for benzoic acid, where a very weak Langmuir equilibrium constant $K = 2 \times 10^3$ M^{-1} was measured.[48,51] Clearly, eosin is not specifically adsorbed on aqueous colloidal TiO_2, and is hardly able to displace amphoteric hydroxyl groups from the surface. The formation of an innersphere surface complex in our experimental conditions can therefore be ruled out. This conclusion is corroborated by the results of Hupp et al. [43] showing that eosin coupling with titanium dioxide is much weaker than in the case of coumarin 343, where chelation of surface Ti(IV) by a salicylate moiety is indeed involved,[52] and is not compatible with the formation of an EO/TiO_2 charge transfer complex. Experiments reported by these authors, however, were carried out in the presence of poly(vinyl alcohol). As it will clearly appear in the followings, PVA perturbs notably

the adsorption of the dye. Thus, conclusions of reference 43 cannot be opposed directly to the interpretation of Ramakrishna and Ghosh.[42] At pH $\leq$ 3, dichlorofluorescein [53] and eosin [37] dyes are predominantly in their neutral protonated form and the solubility of these compounds in water is very small ($<10^{-5}$ M). Hilgendorff and Sundström observed that upon addition of TiO_2 colloids, dye aggregates in suspension break up to allow for adsorption of dye molecules on the oxide surface.[16] The occurrence of such a phenomenon is very likely to constitute the actual rationale of observations reported in reference,[42] which were improperly attributed to the formation of surface CT complexes. It implies that crystals of neutral protonated xanthene dyes are not very stable and that interactions of the molecules with the surface are thermodynamically favorable over their precipitation. The latter requirement, combined with spectroscopic and electrophoretic data, and the tri-dimensional structure of eosin, is indicative of a moderately strong anchoring of the dye, presumably through hydrogen-bonding with the hydroxylated oxide surface. At pH 4, electrostatic forces furthermore drive adsorption of EO monoanions.

Dimer Formation. Figure 2 displays a clear difference between the absorption spectrum of the dye/oxide system and its fluorescence excitation spectrum. This observation precludes the possibility that the shoulder appearing in the absorption feature could be due to the formation of a new type of bond, a modification of the local environment, or a distortion of adsorbed molecules. A different species should thus be involved upon adsorption of eosin, whose fluorescence is weaker than that of the native dye molecule. Eosin and other xanthene dyes tend to form dimers or larger aggregates in concentrated solutions.[54] In water, at concentrations larger than 10^{-4} M, eosin dianions are known to form nonfluorescent dimers, where two chromophores are associated together in a head-to-tail geometry.[55] Protonation of the dye in our experimental conditions decreases the electrostatic repulsion between EO anions and should therefore favor even more this tendency to aggregate. The absorption spectrum of EO dimers displays a doublet with maxima at 485 and 540 nm.[56] As a result, a solution that contains both monomeric and aggregated forms of the dye is characterized by a lower extinction coefficient and an additional spectral shoulder on the blue side of the main absorption peak.[57] The absorption spectrum of eosin adsorbed on Al_2O_3 and TiO_2 colloids closely matches the optical features reported for a 2×10^{-2} M dye solution, where 60% of the eosin molecules are believed to be associated in the form of dimers.[55,56] Dimer formation on the surface in the same proportion will be further evidenced by kinetic considerations in the followings. It should thus be considered as the source of the spectral distortion of the eosin absorption spectrum in our experimental conditions. The fluorescence spectrum of the adsorbed dye, on the other hand, is essentially due to monomeric dye molecules and shows no sign of an emission from eosin excimers. From this observation and the previous discussion about the mode of adsorption of the dye, it is inferred that the formation of dimers takes place most likely through dipole−dipole interaction between two molecules weakly bound to the surface.

Intermolecular Charge Transfer. The transient spectrum of eosin adsorbed on nonreactive alumina, recorded 10 ps after pulsed excitation (Figure 2), shows that a fraction of the initial excited state population was still exhibiting stimulated emission. The other part of the dye excited states already reacted, yielding in particular product species responsible for the positive transient absorption signal measured below 470 nm. The kinetics of these processes is displayed in Figure 6: The stimulated emission of the dye undergoes fast subpicosecond decay. The surviving excited states, amounting to approximately 30% of the initial population, deactivate on a longer 500 ps time scale, corresponding to their natural radiative and nonradiative decay. Similar dynamics was observed with EO/ZrO_2 system. Although the measured time constants differ only slightly, the main difference between both systems resides in the respective contributions of both decay phases. The fast kinetic component represents ca. 77% of the whole SE signal in EO/alumina system and only 52% on zirconia colloids (Table 1). The fast decay part of the stimulated emission in Al_2O_3 colloids exhibits the same temporal behavior as the transient absorbance measured at 480 nm. At this wavelength, transient spectra measured with a nanosecond flash photolysis setup in identical conditions still reveal a major bleaching component more than 5 μs after pulsed excitation, which was completely absent for eosin in solution.[46] The formation of such long-lived products on the surface of the nonreactive oxide can be attributed to intermolecular electron transfer within eosin dimers yielding ($EO^{+\bullet}EO^{-\bullet}$) radical pairs (eq 2)

$$(EO{-}EO) + h\nu \rightarrow (EO{-}EO^*) \quad (1)$$

$$(EO{-}{}^1EO^*) \rightarrow (EO^{+\bullet}EO^{-\bullet}) \quad (2)$$

$$(EO^{+\bullet}EO^{-\bullet}) \rightarrow (EO\text{-}EO) + \nabla + h\nu \quad (3)$$

$$(EO^{+\bullet}EO^{-\bullet}) \rightarrow EO^{+\bullet} + EO^{-\bullet} \quad (4)$$

$${}^3EO^* + EO \rightarrow EO^{+\bullet} + EO^{-\bullet} \quad (5)$$

This photoinduced dismutation reaction is known to occur upon the encounter between a dye excited triplet state and a ground-state species in solution (eq 5) with a rate constant of 3×10^8 M^{-1} s^{-1}.[50] The fast decay of the SE signal and recovery of the absorption at 480 nm on nonreactive oxide surfaces indicate a typical rate constant for electron transfer within eosin excited dimers of 2×10^{12} s^{-1} (Table 1). Assuming a value of 1 nm for the radius of the dimer, the distance between the two EO molecules would be approximately equivalent to the mean intermolecular distance in a solution at a concentration of 2×10^{-1} M. The corresponding second-order rate constant would thus be almost 3 orders of magnitude larger than that of reaction 5. The difference observed in the relative contribution of the fast decaying component of the stimulated emission for both alumina and zirconia (Table 1) can be explained by a larger proportion of molecules forming dimers on the surface of Al_2O_3. The latter colloid is indeed constituted of larger particles compared to the ZrO_2 sol and, consequently, offers a reduced surface area for adsorption of the dye. The dynamics of the semireduced $EO^{-\bullet}$ species formed on alumina colloids was followed by probing at 387 nm, in a spectral region where the singlet state does also absorb light. A fast transition from the singlet excited state to $EO^{-\bullet}$ would be expected following the excitation pulse. However, the similarity of the absorption cross sections of both species at this particular wavelength could explain the steady signal observed for the first few picoseconds. A slow 12 ps lifetime decay was monitored at 387 nm, which mirrors the transient behavior of the signal recorded at 480 nm. This kinetic phase can be attributed to the geminate recombination of radical ion pairs and consequent recovery of the dye ground-state (eq 3). Because long-lived charge separated products are still observable on the ns−μs time scale, solvation and separation of the geminate radicals (eq 4) should compete

with this fast recombination and account for the residual signal measured beyond 0.5 ns in Figure 6.

Electron Injection. On the surface of TiO_2 colloids, the fluorescence of both monomers and dimers is quenched rapidly, and no long-lived stimulated emission is observed. The decay of the SE signal is characterized by a 200 fs time constant, quite similar to that measured for transient absorbance monitored at 480 and 387 nm (Figure 7A, Table 1). The SE signal measured at 600 nm indicates that no observable singlet excited state remains 10 ps after the pulsed excitation. These observations that are in variance with results obtained at the surface of insulating oxide colloids can clearly be attributed to the interfacial electron transfer into the conduction band of TiO_2 from excited states of eosin in both monomeric and dimeric forms (eqs 6, 7). The absorption at 387 nm, however, outlives the excited-state emission, demonstrating that semireduced eosin $EO^{-\bullet}$ is also formed at the surface of the reactive semiconductor. Intermolecular charge-transfer taking place in EO dimers (eq 8) appears therefore to compete with electron injection within a comparable time frame

$$^1EO^*|TiO_2 \rightarrow EO^{+\bullet} + e_{cb}^- (TiO_2) \quad (6)$$

$$(EO-{}^1EO^*)|TiO_2 \rightarrow EO + EO^{+\bullet} + e_{cb}^- (TiO_2) \quad (7)$$

$$(EO-{}^1EO^*)|TiO_2 \rightarrow (EO^{+\bullet}EO^{-\bullet})|TiO_2 \quad (8)$$

$$(EO^{+\bullet}EO^{-\bullet})|TiO_2 \rightarrow EO + EO^{+\bullet} + e_{cb}^- (TiO_2) \quad (9)$$

Considering only the fastest component of 200 fs measured for the decay of the stimulated emission of EO/TiO_2 system, and assuming that the intermolecular charge transfer within dimers is characterized by the same time constant $t = 500$ fs as on the surface of Al_2O_3 and ZrO_2, a rate constant for charge injection of $k_{inj} = 3.8 \times 10^{12}\ s^{-1}$ is obtained. Electron injection process, however, does not reduce actually to a simple exponential kinetics and this simple estimate yields only a rough idea of the fastest injection rate. About 60% of the dye is believed to be associated in the form of dimeric species on TiO_2 colloidal particles. No distinction can be done from our observations between interfacial electron transfer from adsorbed excited eosin monomers and dimers (eqs 6 and 7). Independent experimental evidence of the occurrence of photoinduced charge injection from dimeric eosin was provided by Sayama et al.: The action spectrum of an eosin-sensitized photovoltaic solar cells they reported indeed closely matches the absorption spectrum of the dimer.[58] In aggregated eosin, charge injection competes kinetically with intermolecular electron transfer (eq 8) and implies that only approximately two-thirds of the dye excited states associated in dimers would undergo direct interfacial electron transfer. Indirect injection from $EO^{-\bullet}$ species into TiO_2 conduction band (eq 9) should also be possible. The slowest component of 13 and 19 ps measured at 387 and 480 nm, respectively, corresponds quite well to the decay measured on Al_2O_3 colloids, and attributed to the geminate recombination of charge separated ($EO^{+\bullet}EO^{-\bullet}$) radical pairs. Yet it cannot be excluded that reaction 9 could take place on the same time scale.

Although a unique value of the time constant for electron injection cannot be specified, it is possible to compare the electron transfer (ET) reaction rate with the time scale of vibrational relaxation of the excited state. First experimental evidences of electron injection occurring from hot excited states were reported for strongly coupled Ru(II) polypirydyl dyes on TiO_2 nanocrystalline films[21-23] and alizarin/TiO_2 CT complexes.[12,13] In the present case, vibrational relaxation of the singlet excited state of eosin in water was monitored by recording the stimulated emission signal observed at 600 nm, following excitation of the dye at 500 nm. Because 600 nm analyzing pulses should probe mainly transitions taking place from lowest vibrational state of the excited dye molecule, the rise of the SE signal is expected to be kinetically limited by the rate of population of this level. Kinetic fit of the deconvoluted signal growth yielded two time constants of 85 fs (66%) and 1 ps (34%) (Figure 5, Table 1). Solvent reorganization is likely to contribute in the slower part of this relaxation dynamics. Figure 5 shows that SE signals measured with eosin on TiO_2 and Al_2O_3 colloids were intercepted at about one-third of the amplitude reached in solution. Kinetic analysis of the deconvoluted SE signals yielded single exponential decays and no rise component needed to be taken into account for the fitting. Although adsorption of the dye on oxide particles could possibly affect the vibrational dynamics of its excited state and the intensity of stimulated emission, these observations substantiate the occurrence of electron injection from nonthermalized electronic excited states of eosin. Intermolecular charge transfer within dimers appears as well to occur mainly from hot excited states, in competition with rapid vibrational relaxation.

Effect of PVA. Poly(vinyl alcohol) adsorbs efficiently to oxide surfaces, primarily through hydrogen bonding to hydroxyl groups and linkage of the few nonhydrolyzed acetate functions carried by the macromolecules.[59] The conformation of polymer chains on the surface depends on the number of those carboxylic groups (degree of hydrolysis) and the molecular weight. In our case, the large degree of hydrolysis (98%) and high molecular weight of the polymer are expected to result in a structure forming large loops and tails around oxide nanoparticles.[60] Because essentially nonionic poly(vinyl alcohol) molecules cannot significantly affect the surface charge of TiO_2 particles, the important decrease of the zeta potential observed in the presence of PVA can be interpreted in terms of an outward shift of the shear plane location. Using this concept, an effective thickness of the polymer adlayer of the order of 8 nm was estimated from our electrophoretic data.[61] The absorption spectrum of EO in TiO_2 sols in the presence of poly(vinyl alcohol) closely resembles that of the monomeric dye in aqueous solution (Figure 2B). A red shift of 6 nm is observed upon addition of the polymer that could be explained by the decreased polarity of the dye's environment. Clearly, addition of poly(vinyl alcohol) prevents the formation of EO dimers on the surface of colloidal particles. Such an effect can be understood by a decrease of EO surface concentration and thus by the dissolving of the dye monomers within the polymeric adlayer. Rossetti and Brus noted no significant difference between Raman spectra of eosin adsorbed on unprotected titania particles and in the presence of PVA.[36] Contrarily to the original conclusion of these authors that eosin adsorption is not disturbed by polymeric chains, it can be inferred that interactions between EO anions and PVA macromolecules are essentially due to H bonding and are of the same nature as those existing between EO and surface hydroxyl groups. It results from this discussion that sensitizer molecules are likely to be associated within the PVA adlayer and maintained apart from the solid surface, with a very broad distribution of distances separating the dye from the semiconductor.

A striking effect of PVA upon the electron injection dynamics can indeed be observed in Figure 7B. The development of the characteristic absorption at 480 nm demonstrates that the semioxidized $EO^{+\bullet}$ species is produced by a photoinduced

reaction, which, in the absence of dimers, could only be electron injection into TiO_2 conduction band. Compared to the case of unprotected colloids, interfacial charge transfer in systems containing PVA was slowed by orders of magnitude. The stimulated emission signal measured at 600 nm displays practically a linear dependence upon the logarithm of time over three decades. This relationship indicates an electron tunneling controlled process and can clearly be rationalized in terms of the wide distribution of distances separating the sensitizer molecules from the reactive surface, resulting from the spreading of the dye within the polymer adlayer. The faster component of the multiexponential kinetics is characterized by a time constant of at least 1 ps. Yet, most of the dye singlet excited states appear to extend their lifetime up to more than 100 ps. At longer delay time, it becomes evident that charge injection even competes with natural deactivation of the dye singlet excited state and that intersystem crossing is able to populate the excited triplet. These findings are in good agreement with results published earlier, where a typical time constant of 1 ns was reported for photoinduced charge injection from eosin adsorbed onto PVA-protected TiO_2 colloid and apparent competition between charge injection and triplet formation was observed.[37,39]

The effect of PVA upon interfacial electron transfer dynamics emphasizes the importance of the mode of adsorption of the dye. Weakly bond sensitizer molecules are prone to be moved away over a considerable distance by adsorption of molecules having a stronger affinity for the semiconductor surface. Conversely, hydroxyl groups characterizing the amphoteric surface of the oxide in aqueous medium, and on which eosin anions are believed to be anchored through hydrogen-bonding, set a minimum separation distance between the chromophores and the acceptor states manifold of the solid. This view is supported experimentally by the work of Sundström and coworkers: A characteristic time constant of 300 fs for charge injection in the parent 2′,7′-dichlorofluorescein/aqueous colloidal TiO_2 system was found,[16,40] which is close to the 200 fs figure obtained in the present study for eosin-sensitized sols. On nanocrystalline titania films sintered at high temperature and maintained in anhydrous conditions, the oxide surface is essentially dehydroxylated and anchoring of the dye directly on exposed Ti(IV) sites is made possible. As a result, the electronic coupling associated with charge injection is expected to be stronger, and indeed significantly faster injections were observed (shorter time constant <100 fs) for the same 2′,7′-dichlorofluorescein dye.[41] In the weak coupling limit, an exponential relationship for the distance dependence of the electronic coupling is implicit. Assuming an arbitrary value of the dumping factor $\beta = 1.2$ Å^{-1}, a reduction of the donor−acceptor distance by 2 Å, roughly corresponding to the spacing introduced by terminal −OH groups on the surface, would imply an increase by 1 order of magnitude of the coupling matrix element and thus of the reaction rate constant. This effect can be sufficient for making the system cross the strong coupling limit and for promoting coherent electron-transfer processes.

V. Conclusions

Eosin/colloidal TiO_2 system lent itself to a detailed investigation of the effects of surface interaction upon the dynamics of photoinduced electron transfer from dye excited states into the conduction band of semiconductors. Electrophoretic measurements, combined with spectroscopic data and geometrical considerations, were used to assess the mode of adsorption of the sensitizer on the surface of metal oxide nanoparticles in stable aqueous suspensions. Results demonstrated unambiguously that eosin is not specifically anchored onto aqueous TiO_2 colloidal particles at pH 4. Adsorption of the dye anions through electrostatic interaction and hydrogen-bonding to the surface hydroxyl groups, yet, gives rise to the formation of eosin dimers. Dynamics of photoinduced processes was studied by ultrafast laser pump−probe techniques with sub-100-fs time-resolution. Prompt intermolecular electron transfer was observed to take place in dimers through ^{1}EO*−EO dismutation and to compete kinetically with charge injection. Interfacial ET takes place in approximately equal proportions from dimeric and monomeric dye species. This process is characterized by multiexponential kinetics, with time components extending typically from 200 fs (>50%) up to 1 ps. Vibrational relaxation of eosin singlet excited states was found from stimulated emission experiments to occur within the same time frame, precluding their complete thermalization prior to the reaction. The occurrence of charge injection from various hot vibronic levels, along with a wide distribution of possible geometrical conformations of the loosely bound dye on the surface, are likely to be at the origin of the spreading of the reaction rate constants.

Kinetic results obtained with TiO_2 particles coated by poly(vinyl alcohol) allowed for a clear understanding of the seeming discrepancies found between recent experiments, where PVA was absent, and former ones, in which polymer-protected colloids were used. Dispersion of eosin monomers within a nanometers-thick PVA adlayer yields a broad distribution of distances separating the sensitizer's excited states from the reactive surface. In this situation, kinetic parameters for charge injection in the conduction band of TiO_2 covered a large time span from less than 1 ps to hundreds of picoseconds and were only limited at longer times by radiative and nonradiative decay of the dye excited states.

Results obtained for the eosin-sensitized aqueous titanium dioxide colloids are exemplary of the sensitivity of the dynamics of interfacial electron transfer upon surface and environmental conditions in the weak-coupling case. They highlight the need for a strict control of the mode and geometry of adsorption for the discussion of future reports on ultrafast photoinduced charge injection dynamics.

Acknowledgment. Financial support by the Swiss National Science Foundation (FNRS) and the Swiss Federal Institute of Technology at Lausanne (EPFL) is gratefully acknowledged. We thank Tania Rinaldi for experimental assistance at an early stage of this work and Gábor Benkö (Lund University) and Stefan Haacke (University of Lausanne) for helpful discussions.

References and Notes

(1) Fyson, J. R.; Twist, P. J.; Gould, I. R. Electron-transfer processes in silver halide photography. In *Electron transfer in chemistry*; Balzani, V., Ed.; Wiley-VCH: Weinheim, 2001; Vol. 5, pp 285−378.

(2) Weiss, D. S.; Cowdery, J. R.; Young, R. H. Electrophotography. In *Electron transfer in chemistry*; Balzani, V., Ed.; Wiley-VCH: Weinheim, 2001; Vol. 5, pp 379−471.

(3) Grätzel, M. *Nature* **2001**, *414*, 338−344.

(4) Grätzel, M.; Moser, J. E. Solar Energy Conversion. In *Electron Transfer in Chemistry*; Balzani, V., Ed.; Wiley-VCH: Weinheim, 2001; Vol. 5, pp 589−644.

(5) Marcus, R. A. *Angew. Chem., Int. Ed.* **1993**, *32*, 1111−1121.

(6) Jortner, J. *J. Chem. Phys.* **1976**, *64*, 4860−4867.

(7) Lanzafame, J. M.; Palese, S.; Wang, D.; Miller, R. J. D.; Muenter, A. A. *J. Phys. Chem.* **1994**, *98*, 11020−11033.

(8) Miller, R. J. D.; McLendon, G. L.; Nozik, A. J.; Schmickler, W.; Willig, F. *Surface Electron-Transfer Processes*; VCH: New York, 1995.

(9) Rehm, J. M.; McLendon, G. L.; Nagasawa, Y.; Yoshihara, K.; Moser, J. E.; Grätzel, M. *J. Phys. Chem.* **1996**, *100*, 9577−9578.

(10) Tachibana, Y.; Moser, J. E.; Grätzel, M.; Klug, D. R.; Durrant, J. R. *J. Phys. Chem.* **1996**, *100*, 20056−20062.

(11) Wachtveitl, J.; Huber, R.; Spörlein, S.; Moser, J. E.; Grätzel, M. *Int. J. Photoenergy* **1999**, *1*, 153−155.
(12) Huber, R.; Spörlein, S.; Moser, J. E.; Grätzel, M.; Wachtveitl, J. *J. Phys. Chem. B* **2000**, *104*, 8995−9003.
(13) Huber, R.; Moser, J. E.; Grätzel, M.; Wachtveitl, J. *J. Phys. Chem. B* **2002**, *106*, 6494−6499.
(14) Tachibana, Y.; Haque, S. A.; Mercer, I. P.; Moser, J. E.; Klug, D. R.; Durrant, J. R. *J. Phys. Chem. B* **2001**, *105*, 7424−7431.
(15) Burfeindt, B.; Hannappel, T.; W., S.; Willig, F. *J. Phys. Chem.* **1996**, *1996*, 16463−16465.
(16) Hilgendorff, M.; Sundström, V. *J. Phys. Chem. B* **1998**, *102*, 10505−10514.
(17) Martini, I.; Hodak, J. H.; Hartland, G. V. *J. Phys. Chem. B* **1998**, *102*, 9508−9517.
(18) Asbury, J. B.; Ellingson, R. J.; Ghosh, H. N.; Ferrere, S.; Nozik, A. J.; Lian, T. *J. Phys. Chem. B* **1999**, *103*, 3110−3119.
(19) Asbury, J. B.; Hao, E.; Wang, Y.; Lian, T. *J. Phys. Chem. B* **2000**, *104*, 11957−11964.
(20) Moser, J. E.; Bonhôte, P.; Grätzel, M. *Coord. Chem. Rev.* **1998**, *171*, 245−250.
(21) Moser, J. E.; Grätzel, M. *Chimia* **1998**, *52*, 160−162.
(22) Moser, J. E.; Wolf, M.; Lenzmann, F.; Grätzel, M. *Zeit. Phys. Chem.* **1999**, *212*, 85−92.
(23) Benkö, G.; Kallioinen, J.; Korppi-Tommola, J. E. I.; Yartsev, A. P.; Sundström, V. *J. Am. Chem. Soc.* **2002**, *124*, 489−493.
(24) Zimmermann, C.; Willig, F.; Ramakrishna, S.; Burfeindt, B.; Pettinger, B.; Eichberger, R.; Storck, W. *J. Phys. Chem. B* **2001**, *105*, 9245−9253.
(25) Huber, R.; Moser, J. E.; Grätzel, M.; Wachtveitl, J., to be published.
(26) Tachibana, Y.; Haque, S. A.; Mercer, I. P.; Durrant, J. R.; Klug, D. R. *J. Phys. Chem. B* **2000**, *104*, 1198−1205.
(27) Houlding, V. H.; Grätzel, M. *J. Am. Chem. Soc.* **1983**, *105*, 5695−5696.
(28) Vlachopoulos, N.; Liska, P.; Augustynski, I.; Grätzel, M. *J. Am. Chem. Soc.* **1988**, *110*, 1216−1220.
(29) Blackbourn, R. L.; Johnson, C. S.; Hupp, J. T. *J. Am. Chem. Soc.* **1991**, *113*, 1060−1062.
(30) Gosh, H. N.; Asbury, J. B.; Weng, Y.-X.; Lian, T. *J. Phys. Chem. B* **1998**, *102*, 10208−10215.
(31) Frei, H.; D., F.; Grätzel, M. *Langmuir* **1990**, *6*, 198−206.
(32) Kamat, P. V. *Chem. Rev.* **1993**, *93*, 267−300.
(33) Matsumara, M.; Nomura, Y.; Tsubomura, H. *Bull. Chem. Soc. Jpn.* **1976**, *49*, 1409−1414.
(34) Moser, J. *Monatsh. Chem.* **1887**, *8*, 373.
(35) Kamat, P. V.; Fox, M. A. *Chem. Phys. Lett.* **1983**, *102*, 379−384.
(36) Rossetti, R.; Brus, L. E. *J. Am. Chem. Soc.* **1984**, *106*, 4336−4340.
(37) Moser, J.; Grätzel, M. *J. Am. Chem. Soc.* **1984**, *106*, 6557−6564.
(38) Fleming, G. R.; Knight, A. W. E.; Morris, J. M.; Robinson, G. W.; Morrison, R. J. S. *J. Am. Chem. Soc.* **1977**, *99*, 4306−4311.
(39) Moser, J.; Grätzel, M.; Sharma, D. K.; Serpone, N. *Helv. Chim. Acta* **1985**, *68*, 1686−1690.
(40) Hilgendorff, M.; Sundström, V. *Chem. Phys. Lett.* **1998**, *287*, 709−713.
(41) Benkö, G.; Hilgendorff, M.; Yartsev, A. P.; Sundström, V. *J. Phys. Chem. B* **2001**, *105*, 967−974.
(42) Ramakrishna, G.; Gosh, H. N. *J. Phys. Chem. B* **2001**, *105*, 7000−7008.
(43) Walters, K. A.; Gaal, D. A.; Hupp, J. T. *J. Phys. Chem. B* **2002**, *106*, 5139−5142.
(44) Moser, J.; Grätzel, M. *J. Am. Chem. Soc.* **1983**, *105*, 6547−6555.
(45) Piel, J.; Beutter, M.; Riedle, E. *Optics Lett.* **1999**, *25*, 180−182.
(46) Pelet, S. Femtosecond dynamics of electron transfer in the photosensitization of wide band gap semiconductors. Ph.D. Thesis, EPF Lausanne, Switzerland, 2002.
(47) Reindl, S.; Penzkofer, A. *Chem. Phys.* **1996**, *213*, 429−438.
(48) Moser, J.; Punchihewa, S.; Infelta, P. P.; Grätzel, M. *Langmuir* **1991**, *7*, 3012−3018.
(49) Penzkofer, A.; Beidoun, A.; Speiser, S. *Chem. Phys.* **1993**, *170*, 139−148.
(50) Kasche, V.; Lindquist, L. *Photochem. Photobiol.* **1965**, *4*, 923−933.
(51) Blesa, M. A.; Weisz, A. D.; Morando, P. J.; Salfity, J. A.; Magaz, G. E.; Regazzoni, A. E. *Coord. Chem. Rev.* **2000**, *196*, 31−63.
(52) Weisz, A. D.; Regazzoni, A. E.; Blesa, M. A. *Solid State Ionics* **2001**, *143*, 125−130.
(53) Leonhardt, H.; Gordon, L.; Livingston, R. *J. Phys. Chem.* **1971**, *75*, 245−249.
(54) Valdes-Aguilera, O.; Neckers, D. C. *Acc. Chem. Res.* **1989**, *22*, 171−177.
(55) Förster, T.; König, E. *Zeit. Electrochem.* **1956**, *61*, 344−348.
(56) Rohatagi, K. K.; Mukhopadhyay, A. K. *Photochem. Photobiol.* **1971**, *14*, 551−559.
(57) Toptygin, D.; Packard, B. Z.; Brand, L. *Chem. Phys. Lett.* **1997**, *277*, 430−435.
(58) Sayama, K.; Sugino, M.; Sugihara, H.; Abe, Y.; Arakawa, H. *Chem. Lett.* **1998**, 753−754.
(59) Santhiya, D.; Subramanian, S.; Natarjan, K. A.; Malghan, S. G. *J. Colloid Interface Sci.* **1999**, *216*, 143−153.
(60) Chibowski, S.; Paszkiewicz, M. *J. Dispersion Sci. Technol.* **2001**, *22*, 281−289.
(61) Miller, N. P.; Berg, J. C. *Coll. Surf.* **1991**, *59*, 119−128.